

# Fiber Specklegram Multiplexed Sensor

Luis Rodriguez-Cobo, Mauro Lomer and Jose-Miguel Lopez-Higuera *Senior Member, IEEE*,

**Abstract**—In this work, several multiplexing techniques have been combined to achieve a Fiber Specklegram Multiplexed Sensor (FSMS), continuing the preliminary results presented at OFS23. Using a single CCD camera as detector, two lasers of different wavelengths have been launched into two multimode Polymer Optical Fibers (POFs) and then combined through a 2x2 coupler before their interrogation. Both coupler exit fibers have been projected to different CCD positions and by analyzing each color of the video sequence, the four fiber channels can be independently obtained. In addition, the speckle sensitivity has been also studied analyzing different properties of speckle patterns such as their contrast or the speckle size. The achieved results will be very useful to the development of new fiber specklegram sensors with several sensing areas using only a CCD camera as detector, making possible low cost sensing devices.

**Index Terms**—Optical fiber transducer, Speckle, Multiplexing

## I. INTRODUCTION

The extremely high sensitivity to external perturbations exhibited by Fiber Specklegram Sensors (FSSs) based on multimode fibers can be interesting for many sensing purposes. A speckle pattern (specklegram) can be created by the propagated modes interfering within an optical fiber. Each point of the field distribution (speckle) combines several contributions with aleatory phases and depends on the fiber stability [1] thus, speckle patterns are sensitive to changes on their propagating medium (e.g. optical fiber for FSSs) and can be employed as sensing elements.

Particularly, perturbations applied to optical fibers have influence on phase, polarization and distribution of the modes. By analyzing variations within speckle patterns, different perturbations applied to the medium (e.g. optical fiber) can be extracted giving rise to sense different perturbations such as: vibration [2], displacement [3], angular alignment [4], strain [5], [6] and even vital signs [7].

Although the interference process of speckle patterns within multimode fibers can be complex and difficult to model, recent advances on computation technologies allow real-time video processing schemes that simplify the extraction of useful information from raw specklegrams, achieving low cost sensing systems. An example of these new approaches is a spectrometer able to obtain a final resolution of 10 *pm* employing the correlation of speckle patterns [8] or using a webcam to study the blood flow based on laser speckle contrast imaging [9].

FSSs have been proved as very sensitive systems that can be implemented using low-cost technologies. However, within

typical FSSs, a CCD is located at the output end of the fiber to record the images with the distribution of the optical field, what limits the number of sensors. Trying to overcome this limitation, a Fiber Specklegram Multiplexed Sensor (FSMS) has been recently presented at OFS23 [10] where two channels have been achieved using a single CCD color camera. In this work, these preliminary results have been completed with other multiplexing techniques to increase the number of sensing areas within FSSs, achieving new results.

## II. SPECKLE SENSITIVITY

Multimode optical fibers are capable of guiding a great amount of propagating modes, each one with a different phase velocity. Based on the geometrical optics approximation, rays are propagated within the optical fiber core with different angles. These angular variations provoke differences on travel paths, which gives rise to phase delays at the fiber exit between the propagated modes that may interfere depending on the source coherence.

After projecting the beam of a multimode fiber, a grainy circular pattern can be observed when the light source is coherent: this is known as speckle pattern (specklegram) and it is composed by a lot of individual speckles (bright dots and dark areas). The intensity of each individual speckle may vary while the total intensity of the speckle pattern must remain constant. These variations can be produced by slow changes on the fiber (thermal, refraction index...) or by an external perturbation, produced on any point of the fiber.

An exact model of speckle pattern variations can be very complex to be develop because there is a great amount of parameters to determine. However, an approximated relation between perturbations and the variations of speckle patterns can be directly obtained to get information regarding the applied perturbation, simplifying the final model. From a sensing point of view, the ultimate goal would be to determine the sensor sensitivity to some parameters, and it is strongly driven by the specklegrams sensitivity itself.

In summary, the sensitivity of a typical fiber specklegram sensor is basically given by the amount and contrast of the dots (individual speckles) comprised within the captured images [1]. These two values are mainly influenced by three factors: the light source, the multimode fiber and the detecting device (usually a CCD camera):

- 1) **Light source:** Speckle patterns are produced by coherent light sources and their contrast is related to the coherence length of the source ( $L_c$ ). The final sensitivity is directly related to speckle contrast thus, consequently, higher sensitivities are achieved with more coherent

This work has been supported by the project TEC2013-47264-C2-1-R

The authors are with the Photonics Engineering Group of Universidad de Cantabria, Santander, 39005, Spain. e-mail: luis.rodriguez@uican.es

light sources. This phenomenon has been employed [11], [12] to analyze some properties of laser sources measuring the contrast of the generated speckle patterns. On the other hand, speckle patterns also change with wavelength. Two speckle patterns created by launching two sources with different wavelengths within the same optical fiber will have different spatial positions. Particularly, this effect has been recently employed to build a spectrometer able to obtain a final resolution of 10 *pm* employing the correlation of speckle patterns [13].

- 2) **Optical fiber:** Since speckle patterns are created by interference of the propagated modes within a multimode optical fiber, the amount of individual speckles can be considered approximately proportional to the number of propagated modes. Therefore the number of speckles can be calculated [1] using  $N_s \approx (2a \cdot \pi \cdot NA/\lambda)^2$ , where  $2a$  is the core diameter,  $NA$  is the numerical aperture and  $\lambda$  the wavelength of the laser source. For example, if every mode is propagated within a multimode optical fiber of 1 *mm* core diameter and  $NA = 0.5$  using a He-Ne laser ( $\lambda = 0.6328 \mu m$ ), the number of speckles is approximately  $N_s \approx 6.2 \cdot E6$ .

Since specklegram sensors [6] usually analyze the intensity variations of each individual speckle dot, for the same speckle pattern intensity, the sensor sensitivity increases with the number of individual speckles comprised within the pattern. Based on the previous approximation, for a given optical fiber the number of speckles is inversely proportional to the wavelength thus, consequently, the sensor sensitivity is also inversely proportional to the wavelength.

- 3) **Detector:** One of the best options to detect speckle patterns are commercial CCD color cameras. This detector can record each specklegram over time and determines the final sensor response. Three main characteristics are usually considered in a CCD: resolution, detecting area and dynamic range. Although these parameters have their influence on the system sensitivity, they are more related to the experimental setup than to the speckle phenomenon. For example, the resolution and detecting area are directly related to the distance between the fiber end and the camera, as well as the dynamic range (by increasing this distance, the intensity projected to the CCD decreases). Nowadays, there are low-cost CCD cameras (e.g. webcams) with enough performance to obtain high precision measurements and reduce the final cost of the sensor system [9].

Employing a single detection device (e.g. CCD) and apart from the mechanical properties of the sensing fibers (that do not depend on the optical properties), the final sensor sensitivity is strongly driven by the source properties and can be summarized into three main speckle pattern properties:

- **Contrast** ( $C_s$ ), that is directly related to the coherence length ( $L_C$ ) of the laser source.
- **Number of speckles** ( $N_s$ ), that is inversely related to the square value of wavelength ( $\lambda$ ).
- **Intensity** ( $I_s$ ), that scales the speckles' differences and

is related to the incoming power and to the detector.

Employing several metrics on analyzed speckle patterns and using the same detecting device and resolution and also maintaining the multimode fiber, the final sensor sensitivity can be expressed as a function of:

$$S_{Speckle} \propto I_s \cdot C_s \cdot N_s \propto I_s \cdot \frac{L_C}{\lambda^2} \quad (1)$$

This simplification assumes that the total intensity of the speckle pattern remains constant during the applied perturbations. The best approach is to record the whole speckle pattern to guarantee this condition; however, having enough individual speckles within captured specklegrams may be sufficient for this requirement, simplifying the sampling requirements.

### III. MULTIPLEXING TECHNIQUES

FSSs, in combination with CCDs, have been proved as a very sensitive solution at reduced costs [5] however, a simple FSS system employs a CCD for each sensing point [6], what limits their application to multi-point sensing scenarios. In this work, different multiplexing schemes have been proposed to overcome this limitation, particularly wavelength-division and space-division have been studied for these purposes.

#### A. Wavelength division multiplexing (WDM)

Based on a CCD color camera as sensing device, up to three simultaneous channels can be obtained employing different laser sources, each one matching a single color of the RGB detector. Main contributions to sensitivity, summarized in section II, have to be considered on the final performance, given that this multiplexing scheme employs several lasers with different wavelengths to discriminate between speckle patterns. Each filter of a standard color camera can isolate a speckle pattern produced by a laser, enabling up to three different channels using a single CCD.

However, since the speckle sensitivity is affected by the total intensity of the speckle pattern (Eq. 1), each filter within the RGB camera has to be compensated to avoid differences on the detected specklegram intensity. Besides, commercial CCDs usually employ wide RGB filters that can produce cross-talk depending on the chosen laser sources, which can also introduce some noise.

#### B. Space division multiplexing (SDM)

This scheme takes advantage of the whole CCD area by projecting different speckle patterns over the whole CCD. However, the total intensity of the speckle pattern must remain constant to obtain reliable measurements thus, consequently, the whole size of specklegrams captured at different CCD positions must contain enough speckles to achieve this requirement. Therefore, the area of each CCD section will be limited by the specklegram diameter and also by the resolution of the CCD.

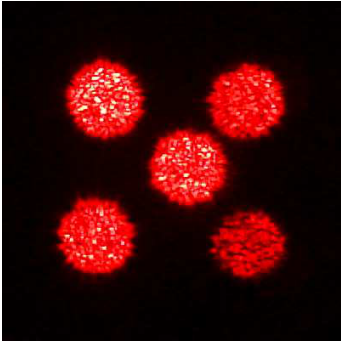


Fig. 1: Five speckle patterns have been projected to the same CCD area. Each specklegram has been produced by a POF of  $50\mu\text{m}$  diameter using a He-Ne laser.

In Fig. 1 five sensing areas have been created into the same CCD by projecting specklegrams of different multimode optical fibers. Each specklegram contains enough speckles to maintain the speckle pattern intensity during the perturbations. The ultimate goal when working with spatial division is to allocate different specklegrams with enough speckles to keep the total intensity constant and also with enough resolution without saturating the CCD.

#### IV. EXPERIMENTS

Both multiplexing techniques, WDM and SDM, have been studied to identify specific problems of each approach. Since the spatial division only requires special attention to the CCD resolution and projected intensity (to avoid CCD saturation), a dedicated setup has been employed to analyze the performance of WDM specklegram sensors. In the following, both approaches have been employed in a different experiment to analyze their combined response.

##### A. Wavelength division multiplexing setup

This scheme relies on launching two different laser sources, each one centered on a RGB filter of the CCD camera, trying to avoid cross-talking. Particularly, two very different lasers have been employed: a cheap laser diode centered on 532 nm and a He-Ne laser emitting at 632.8 nm. Differences between laser sources (particularly their coherence length), allow a better understanding of the factors that exhibit influence on the sensor sensitivity.

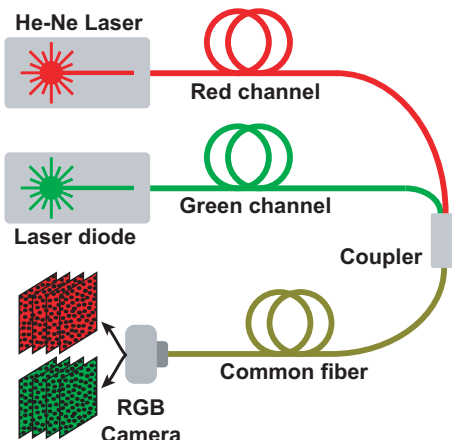


Fig. 2: Two lasers are launched into two POFs and combined using a coupler. This combination is attached to a commercial CCD camera for the interrogation.

Both lasers were launched into different POFs (1 m length and  $980\mu\text{m}$  of core diameter) and then combined using a 50-50 coupler. The common fiber was connected to a single RGB camera to record the speckle patterns. The experimental setup is depicted in Fig. 2.

The power difference between channels, caused by different laser sources, asymmetric coupling and losses of RGB filters of CCD, has been compensated by scaling each one of the employed channels (Red and Green) by its mean value. In Fig. 3 (a), a captured specklegram of 400 by 400 pixels is depicted. The intensity of both channels (Red and Green) has been equalized to compensate the influence of laser power and RGB filtering (Fig. 3, b). Both isolated channels are also depicted in Fig. 3 (c,d).

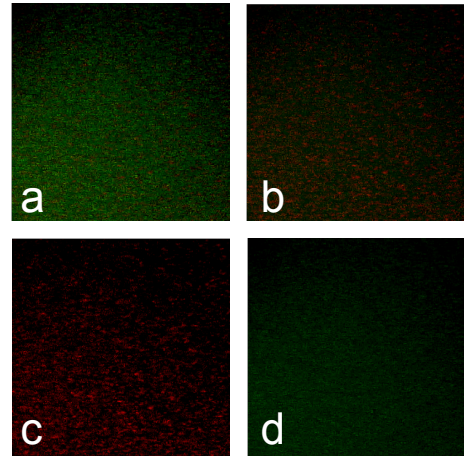


Fig. 3: Captured specklegram of 400 by 400 pixels (a). The same specklegram has been equalized to compensate the power difference between channels (b). Red (c) and green (d) channels have been isolated.

1) *Contrast analysis:* The visibility of speckles (given by the coherence of the source) has a great influence on the final sensitivity of the sensor. Trying to experimentally verify this assumption, the contrast of both channels has been obtained. Since the areas of lower intensity of the speckle patterns are not detected with the employed setup, the RMS contrast [10] has been used to determine the quality of the chosen lasers. This metric can be defined as:

$$C_{RMS} = \sqrt{\frac{1}{MN} \sum_{n=0}^{N-1} \sum_{m=0}^{M-1} (I_{nm} - \bar{I})^2} \quad (2)$$

where intensities  $I_{nm}$  are the  $n$ -th  $m$ -th element of the two dimensional specklegram of size  $M$  by  $N$ .  $\bar{I}$  is the average intensity of all pixel values of the specklegram.

Particularly, for the speckle patterns depicted in Fig. 3 (c,d), the achieved RMS contrast was  $C_R \approx 0.06$  and  $C_G \approx 0.03$  for red and green channels respectively. As expected based on the coherence length of the employed sources (several meters for the He-Ne versus a few millimeters for the cheap laser diode), the red specklegram offers a better contrast than green.

2) *Differential processing scheme*: A simple differential processing scheme has been chosen for this application, trying to isolate the sensitivity dependence with the speckle contrast and wavelength. This scheme is based on computing the differences between two consecutive specklegrams. This is usually more sensitive to quick variations and remove several noises (e.g. thermal effects) because it is insensitive to slow perturbations. A differentially processed sequence for two specklegrams of  $N \times M$  pixels can be defined as

$$\Delta I_D\{i\} = \frac{1}{K \cdot MN} \sum_{n=0}^{N-1} \sum_{m=0}^{M-1} |I_{nm}^{i-1} - I_{nm}^i| \quad (3)$$

where  $K$  is the full scale value of the specklegram color map (e.g.  $K = 255$  for 8-bit grayscale) and  $I_{nm}^i$  corresponds to the pixel of the  $n, m$  position of the  $i$ -th specklegram.

There is a model [2] that determines a proportionality between speckle pattern variations and the perturbation to be measured [5], [6]. This model is limited to small perturbations and can be combined to the differential processing scheme, because between two consecutive specklegrams the applied perturbation should be small.

3) *Results*: Employing the setup depicted in Fig. 2, different mechanical perturbations have been applied to both fibers. Several initial tests have been performed to determine the influence of the cross-talk between different channels of the RGB camera. By switching off one laser, the signal was analyzed in both channels, with and without perturbation on the individual fibers. The achieved results proved the absence of cross-talk, on the employed setup, simplifying the processing scheme. The same perturbations have been applied to the individual fibers and to the common one. Some of the achieved results are depicted below:

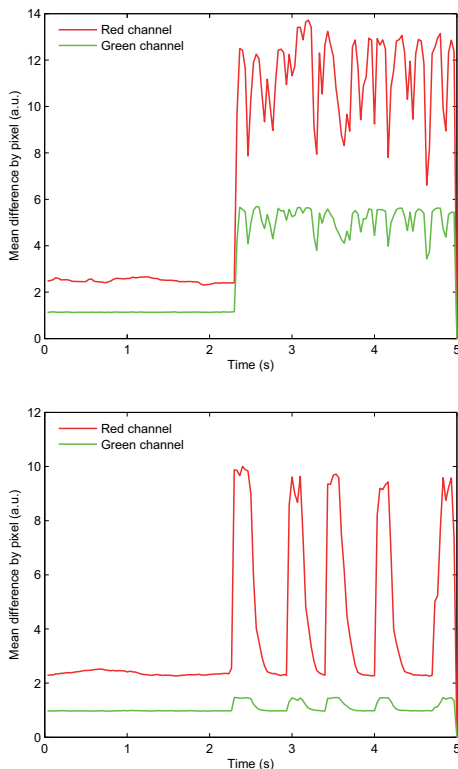


Fig. 4: Differential processed sequences of red and green channels under a perturbation on the common fiber (top) and on the red fiber (bottom).

In Fig. 4 (top), the differential processed sequence of each channel is depicted when an external perturbation was applied to the common fiber. After equalizing the power between channels, the red channel exhibits a higher sensitivity than the green, as the contrast analysis pointed out. The red contrast is two times higher than the green, which is higher than wavelength influence (around 30% of sensitivity increment). In Fig. 4 (bottom), the perturbation was just applied to the red fiber however, some slight perturbations were superficially transmitted to the green fiber through the fixing table and it can be noticed, proving the extreme sensitivity of fiber specklegram sensors.

### B. Space and wavelength division multiplexing setup

This experiment combines both multiplexing techniques SDM and WDM described in section III to increase the number of channels offered to a single detection device. Since the employed laser sources have been maintained, their wavelength and contrast properties have been also kept. As it occurred in the previous setup, both lasers were launched into different POFs (1 m length and  $980 \mu m$  of core diameter) and then combined using a 50-50 coupler, but this one had two output fibers, which have been connected to the same CCD camera but projected to different CCD locations. The chosen fibers produce very small speckles thus, as happened in the previous setup, the fiber end must be distanced from the CCD to enlarge the speckle size and to have enough resolution for the interrogation. In this case, an opaque separation has been introduced between fibers to isolate both spatial channels. The final setup is depicted in Fig. 5.

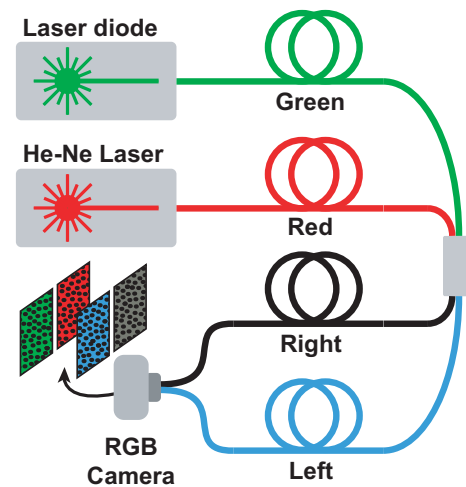


Fig. 5: Two lasers are launched into two POFs and combined using a coupler. Both outputs have been projected to the same CCD but at different locations.

The described setup can be divided into four sensing areas as detailed in Fig. 5 and from the detecting device, also four

channels can be recovered (red and green channels and also left and right ones). As happened previously, the intensity of each channel has been normalized to remove this dependence from the sensitivity.

The system depicted in Fig. 5 defines four sensing areas: two coming from both lasers and two projected at different CCD locations. Also four channels can be separated at the detector side: Left-Red (LR), Left-Green (LG), Right-Red (RR) and Right-Green (RG), whose intensity variations can be defined as the combination of two isolated intensity variations:

$$\begin{aligned}\Delta I_{LR} &= \Delta I_{Left} + \Delta I_{Red}; \\ \Delta I_{LG} &= \Delta I_{Left} + \Delta I_{Green}; \\ \Delta I_{RR} &= \Delta I_{Right} + \Delta I_{Red}; \\ \Delta I_{RG} &= \Delta I_{Right} + \Delta I_{Green};\end{aligned}\quad (4)$$

being each isolated intensity variation (e.g.  $\Delta I_{Green}$ ) matched to a sensing section as described in Fig. 5. The total intensity of each sensing channel has been normalized to compensate the different sensitivities.

1) *Referenced processing scheme*: An absolute referenced processing scheme has been chosen to deal with these experiments. Instead of the differential scheme, this method increases the sensitivity of the whole system (and also the noise) because slow variations within speckle patterns can be also detected. Computationally, it is almost the same method but the reference remains constant. It can be defined as:

$$\Delta I_R\{i\} = \frac{1}{K \cdot MN} \sum_{n=0}^{N-1} \sum_{m=0}^{M-1} |I_{nm}^i - I_{nm}^{Ref}| \quad (5)$$

where  $I_{nm}^{Ref}$  is the intensity of the  $n, m$  pixel of the reference specklegram. The selection of the reference specklegram limits the final performance of the whole system, due to its limitations regarding its dynamic range [5]. For these experiments, the reference specklegram has been captured just before the perturbations to ensure working within a close range. The model described in [2], can be also applied in this scenario, obtaining variations within speckle pattern intensities proportional to the perturbation.

2) *Correlation*: Processing the four detected channels (LR, LG, RR and RG) using the referenced scheme (Eq. 5), four sequences are obtained. According to Eq. 4, each sequence combines the perturbation of two independent channels thus, it is necessary to obtain the common signal between the intensity variations of different channels to extract the perturbation applied to each sensing area. Taking a window size of  $W$  samples, the correlated value for the left channel can be defined as:

$$\Delta I_{Left}\{i\} = \frac{1}{W} \cdot \sum_{w=0}^{W-1} |\Delta I_{LG}\{i+w\} \cdot \Delta I_{LR}\{i+w\}| \quad (6)$$

According to Eq. 4 and 6, the intensity variation of each sensing area can be extracted by correlating different pairs of processed sequences. For this specific scenario, the window size has been set to  $W = 10$  samples that represents a sampling time of  $T_s \approx 0.3s$ .

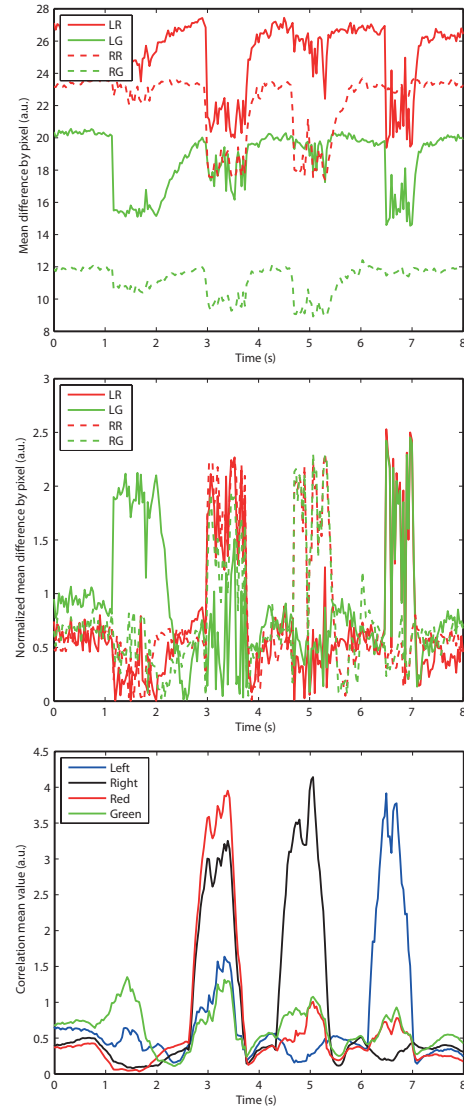


Fig. 6: Processed specklegram sequences (top), sensitivity normalization (middle) and correlation results (bottom).

3) *Results*: Based on the setup described in Fig. 5, some experiments have been proposed to test the demodulation scheme. Each of the four sensing areas (Green, Red, Left and Right fibers) has been individually perturbed to analyze the demodulation scheme. As explained in previous sections, there are many factors that contribute to the sensitivity of a fiber specklegram sensor (coherence length, wavelength...). However, in this scenario, a perturbation has been applied to each sensing area, being detected by two detecting channels. Thus, the same perturbation is scaled with different sensitivities, what provokes errors in their direct correlation. The intensity variations of detected channels have been normalized using their standard deviation to make the sensitivity of each channel directly comparable, dealing with this sensitivity problem.

In Fig. 6 (top), the four referenced processed sequences and the four scaled sequences that compensate sensitivity differences (middle) are depicted. When a perturbation is applied, at least two sequences reflect some variations. However, this data is not intuitive because of the noise and the combination of different signals. The correlated sequences have been also

computed and are depicted in Fig. 6 (bottom), where each sensing area has its own correlated sequence. The achieved results exhibit a good demodulation on spatial channels. A clear peak can be observed on *Left* and *Right* sequences when the perturbation was applied to their corresponding sensing areas. On the contrary, in terms of wavelength demodulation, the *Green* channel does not exhibit a clear peak when a perturbation was applied to its sensing area. Besides, the *Right* channel becomes active when the perturbation is on the *Red* channel sensing area. These problems can be explained by the differences between laser properties, particularly the coherence length.

The green laser diode has a very small coherence length in comparison to the He-Ne, what can be observed in the contrast of their associated speckle patterns. Beyond the sensitivity dependence to this parameter, having smaller coherence length implies that the detected perturbations fade faster as modes propagate through the fiber. Speckle patterns provoked by low coherent sources fade faster during their propagation and can be easily masked by other perturbations produced close to the fiber end. For this scenario, this effect is only noticed for the green laser, explaining the absence of its associated perturbation peak.

On the contrary, the *Right* channel becomes active during the *Red* channel perturbation and this is produced because there is enough correlation between *Right* and *Left* channels. As happened in the previous experiment (Fig. 4), some small mechanical perturbations are also applied to the *Left* channel during the *Red* perturbation. This noise, in addition to the great sensitivity exhibited by the red laser source, creates this “virtual” perturbation on the *Right* detection area, pointing out the importance of employing similar laser sources for WDM techniques.

## V. CONCLUSIONS

In this work, two multiplexing schemes (wavelength and space division) have been employed to increase the number of sensing areas of FSSs using a single CCD camera as detector. Several proof-of-concept setups have been also employed to analyze different parameters of the final sensitivity that have influence on demultiplexing. The achieved results point out the importance of employing similar laser sources (mainly limited by their coherence) to achieve good results after demultiplexing, increasing the benefits of FSMSs for multi-point sensing systems.

## REFERENCES

- [1] J. W. Goodman, *Speckle phenomena in optics: theory and applications*. Roberts and Company, 2007, vol. 1.
- [2] W. Spillman Jr, B. Kline, L. Maurice, and P. Fuhr, “Statistical-mode sensor for fiber optic vibration sensing uses,” *Applied optics*, vol. 28, no. 15, pp. 3166–3176, 1989.
- [3] F. T. Yu, M. Wen, S. Yin, and C.-M. Uang, “Submicrometer displacement sensing using inner-product multimode fiber speckle fields,” *Applied optics*, vol. 32, no. 25, pp. 4685–4689, 1993.
- [4] S. Yin, P. Purwosumarto, and F. T. Yu, “Application of fiber specklegram sensor to fine angular alignment,” *Optics communications*, vol. 170, no. 1, pp. 15–21, 1999.
- [5] Z. Zhang and F. Ansari, “Fiber-optic laser speckle-intensity crack sensor for embedment in concrete,” *Sensors and Actuators A: Physical*, vol. 126, no. 1, pp. 107–111, 2006.
- [6] L. Rodriguez-Cobo, M. Lomer, A. Cobo, and J.-M. Lopez-Higuera, “Optical fiber strain sensor with extended dynamic range based on specklegrams,” *Sensors and Actuators A: Physical*, vol. 203, pp. 341–345, 2013.
- [7] M. Lomer, L. Rodriguez-Cobo, P. Revilla, G. Herrero, F. Madruga, and J. Lopez-Higuera, “Speckle pattern sensor for detecting vital signs of patients,” in *OFS2014 23rd International Conference on Optical Fiber Sensors*. International Society for Optics and Photonics, pp. 91 5721–91 5721–4.
- [8] B. Redding and H. Cao, “Using a multimode fiber as a high-resolution, low-loss spectrometer,” *Optics letters*, vol. 37, no. 16, pp. 3384–3386, 2012.
- [9] L. M. Richards, S. Kazmi, J. L. Davis, K. E. Olin, and A. K. Dunn, “Low-cost laser speckle contrast imaging of blood flow using a webcam,” *Biomedical optics express*, vol. 4, no. 10, pp. 2269–2283, 2013.
- [10] L. Rodriguez-Cobo, M. Lomer, A. Cobo, E. Real, and J. Lopez-Higuera, “Wavelength domain multiplexed fiber specklegram sensor,” in *OFS2014 23rd International Conference on Optical Fiber Sensors*. International Society for Optics and Photonics, pp. 91 579K–91 579K–4.
- [11] M. Imai and Y. Ohtsuka, “Speckle-pattern contrast of semiconductor laser propagating in a multimode optical fiber,” *Optics communications*, vol. 33, no. 1, pp. 4–8, 1980.
- [12] P. Hlubina, “Spectral and dispersion analysis of laser sources and multimode fibres via the statistics of the intensity pattern,” *Journal of Modern Optics*, vol. 41, no. 5, pp. 1001–1014, 1994.
- [13] B. Redding, S. M. Popoff, and H. Cao, “All-fiber spectrometer based on speckle pattern reconstruction,” *Optics express*, vol. 21, no. 5, pp. 6584–6600, 2013.